V European Conference on Computational Fluid Dynamics
ECCOMAS CFD 2010
J. C. F. Pereira and A. Sequeira (Eds)
Lisbon, Portugal,14-17 June 2010

DIRECT NUMERICAL SIMULATIONS OF IMPULSIVELY STARTING FLOWS FROM CYLINDRICAL AND CONICAL NOZZLES

Ionut Danaila*, Marius-Gabriel Cojocaru† and Sterian Danaila††

*UPMC Univ Paris 06, UMR 7598, Laboratoire Jacques-Louis Lions
4 Place Jussieu, F-75005 Paris, France
e-mail: danaila@ann.jussieu.fr
†CORIA, UMR 6614, Université de Rouen
76801 Saint Etienne du Rouvray, France
e-mail: cojocarm@coria.fr
††Faculty of Aerospace Engineering, Politehnica University
Calea Grivitei 132, Bucharest, Romania
e-mail: s_danaila@aero.pub.ro

Key words: DNS, spherical coordinates, cylindrical coordinates, finite differences, starting flows, vortex ring.

Abstract. *We present two different numerical approaches to simulate flows resulting from the sudden injection of fluid in a quiescent surrounding. The incompressible Navier-Stokes equations are discretized using cylindrical coordinates in the first numerical code and spherical coordinates in the second. The two approaches are well adapted for such simulations, since the axisymmetry of the flow is assumed. High-resolution direct numerical simulations are used to assess for the grid influence on the physical properties of the simulated flows (vortex rings and jets). We quantify the influence of the coordinate system on numerical results, when this is not aligned with the main flow direction (*i.e. *the simulation of the conical injection flow using cylindrical coordinates, or the simulation of the parallel injection flow using spherical coordinates).*

1 INTRODUCTION

Flows resulting from the sudden injection of fluid in a quiescent surrounding are encountered in numerous practical applications, ranging from combustion to bio-mechanics, and synthetic jet actuators. A striking feature of these flows is the formation of a vortex ring traveling at the tip of the injection plug. The vortex ring dominates the flow and has a strong influence on the subsequent phenomena of practical interest for engineering applications, e.g. the ignition of a combustible mixture in an internal combustion engine.

Even though the vortex ring has been studied for at least one hundred years, the development of modern experimental and numerical tools allowed to put into evidence new phenomena (e.g. the 'formation number' of the vortex ring[1]) and refine basic evolution laws of this fundamental flow. In particular, direct numerical simulations were systematically used to support recent experimental or theoretical investigations on the vortex ring formation[2], post-formation[3], circulation and trajectory[4], mixing[5], transport and stirring[6], etc.

Vortex rings are usually generated in laboratory by a piston/cylinder arrangement. A column of fluid is pushed by a piston into a quiescent surrounding and the boundary layer at the edge of the cylinder separates and rolls-up into a vortex ring. The flow is assumed to be axisymmetric and thus naturally described in cylindrical coordinates (r, ϕ, z).

In a recent paper[3] we used a Navier-Stokes solver in cylindrical coordinates to study the postformation evolution of a laminar vortex ring. High resolution axisymmetric simulations allowed to correct the apparent discrepancy between different experimental[7] and theoretical studies reporting power-laws for the mathematical description of the evolution of translation velocity and integrals of motion (circulation, impulse and energy). In a subsequent contribution[8], we showed that accurate numerical simulations of laminar vortex rings can be performed without computing the flow inside the vortex ring generator. Such simulations used a new analytic model prescribing the discharge velocity at the exit section of the cylindrical vortex generator.

The purpose of the present contribution is to extend our previous numerical studies from cylindrical to conical vortex generators. We consider starting flows issuing from a static diverging conical nozzle. Such flows could still be simulated using a numerical solver in cylindrical coordinates by prescribing appropriate inflow velocity boundary conditions (as usually, the nozzle is not included in the computational domain). A different approach is to use spherical coordinates (R, θ, ϕ) that allows to have a grid naturally aligned with the main (diverging) direction of the flow. The grid adaptivity is thus acquired before simulation, unless usual dynamic adaptivity enforced during the calculation. Figure 1 depicts how the computational domain results from the intersection between the shell defined by two surfaces ($R = const$) and the cone starting from the center of the sphere with a fixed opening angle. The advantage of this approach is that a constant step discretization is able to follow the streamwise spreading of the flow; a well-balanced resolution of the flow field is thus obtained with a reasonable number of grid points.

The idea to use spherical coordinates for the simulation of starting flows from round nozzles is quite original and was integrated by B. J. Boersma in a Navier-Stokes solver that was successfully used to simulate different types of round jets[9,10,11,12]. This solver (hereinafter denoted by SPH-code) will be used in the present study and compared to our solver using cylindrical coordinates (CYL-code).

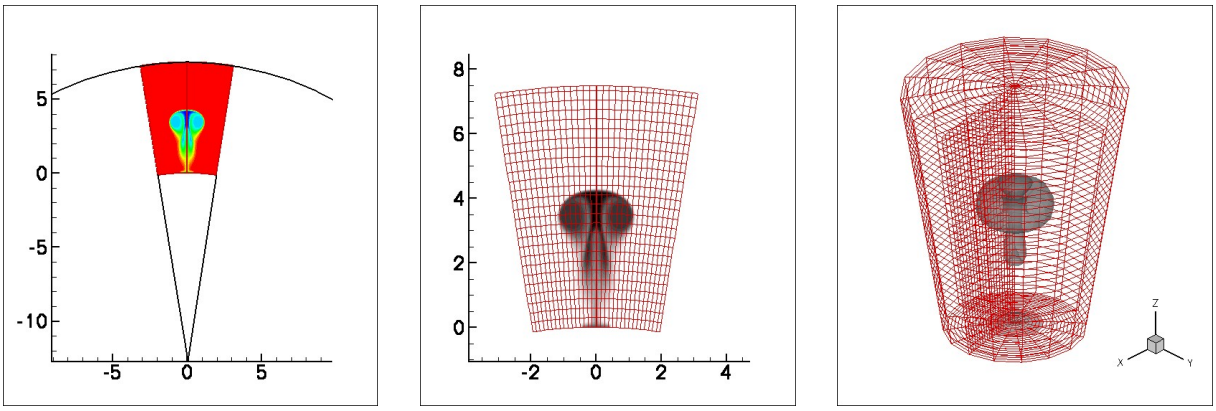

Figure 1: Details of the computational domain for the simulation using spherical coordinates.

Starting from the idea that one usually possesses a single numerical code, we use in this paper high-resolution DNS to assess for the grid influence on the physical properties of the simulated flows (vortex rings and jets). We report for the first time, to our best knowledge, the influence of the coordinate system on the results when this is not aligned with the main flow direction. We therefore consider in the following the simulation of the conical injection using cylindrical coordinates and, respectively, the simulation of the parallel injection using spherical coordinates.

2 NUMERICAL METHOD AND INFLOW BOUNDARY CONDITIONS

The two numerical codes use similar key ingredients. The incompressible Navier-Stokes equations are discretized by centered second-order finite differences on a staggered grid. In the CYL-code, the equations are written in primitive variables $(r \cdot v_r, v_\phi, v_z)$ to avoid the problem of the singularity introduced by the axis[13]. For the time advancement, an explicit Adams-Bashfort scheme is used in the SPH-code and a semi-implicit fractional-step method[14,15] in the CYL-code. The momentum equations are first integrated using an explicit treatment of the pressure gradient. The resulting non-solenoidal field is corrected to satisfy the continuity equation by solving a Poisson equation. The Poisson solver uses a fast Fourier transform following the azimuthal direction and an effective cyclic reduction method (Fishpack subroutines) for solving the remaining two-dimensional system. In both codes, the numerical method is globally second-order accurate in space and time.

For the purpose of this paper, we use both numerical codes to perform axisymmetric

direct numerical simulations of a laminar starting flow. Since the vortex generator will not be simulated, we prescribe the inflow velocity at the inlet of the computational domain. In cylindrical coordinates, the specified discharge velocity (SDV) profile reads:

$$V_z(t,r) = V_0(t)\, V_{zb}(r), \tag{1}$$

where $V_0(t)$ is the 'velocity program' proposed by James and Madnia[16] to describe the piston motion

$$V_0(t) = \begin{cases} \dfrac{U_0}{2}\left\{1+\tanh\left[\dfrac{5}{\tau_1}\left(t-\tau_1\right)\right]\right\}, t \le \tau_1+\tau_2/2 \\ \dfrac{U_0}{2}\left\{1+\tanh\left[\dfrac{5}{\tau_1}\left(\tau_1+\tau_2-t\right)\right]\right\}, t > \tau_1+\tau_2/2, \end{cases} \tag{2}$$

and V_{zb} is the classical hyperbolic tangent profile, which matches very well the shape of profiles measured in experiments (see e.g. Michalke[17]):

$$V_{zb}(r) = \frac{1}{2}\left\{1+\tanh\left[\frac{1}{2\delta_\omega}\left(\frac{D_j}{2r}-\frac{2r}{D_j}\right)\right]\right\}. \tag{3}$$

The parameter δ_ω is the dimensionless thickness of the vorticity layer at the inlet, *i.e.* $\delta_\omega = U_0 D_p / \|\partial V_z/\partial r\|_{max}$. The constants τ_1 and τ_2 separate the three parts in the piston motion: acceleration for $t \in [0, \tau_1[$, velocity plateau $V_0 = U_0$ for $t \in]\tau_1, \tau_2]$ and deceleration for $t \in]\tau_2, t_{\text{off}}]$. At t_{off} the axial velocity becomes zero in the entire inlet section.

In the following, all presented quantities will be normalized using as length and velocity scales the diameter D_j of the vortex generator at the exit section, and, respectively, the bulk velocity U_0. The corresponding reference time is thus D_j/U_0. The main physical parameter of the flow is the Reynolds number based on the characteristic velocity, $Re = U_0\, D_j/\nu$. We set $Re = 1500$, $\delta_\omega = 1/80$ for all simulations.

In the simulations using the SPH-code, the axial velocity U (see Fig. 2) is prescribed using the model (1), with r replaced by the curvilinear coordinate $s = R_0\theta$, where θ is the colatitude and R_0 the radius of the inner shell. The computational domain in Fig. 2 is built by imposing the vortex generator diameter D_j and the (conical injection) angle θ_j. The equivalent velocity profile for the simulations using the CYL-code is obtained by simply imposing the streamwise and radial velocity components as $V_z = U\cos\theta$ and $V_r = U\sin\theta$, respectively. The velocity profiles for the simulations using cylindrical coordinates are also displayed in Fig. 2. For very small values of θ_j we recover the velocity profile (1) that is commonly used to model the exit section of a cylindrical vortex generator[3,8].

At the downstream boundary, a convective[18] boundary condition is applied, enforced by a global mass conservation procedure[19]. The lateral boundary is modeled as a slip-wall in the CYL-code, while flow entrainment[20] is allowed in the SPH-code.

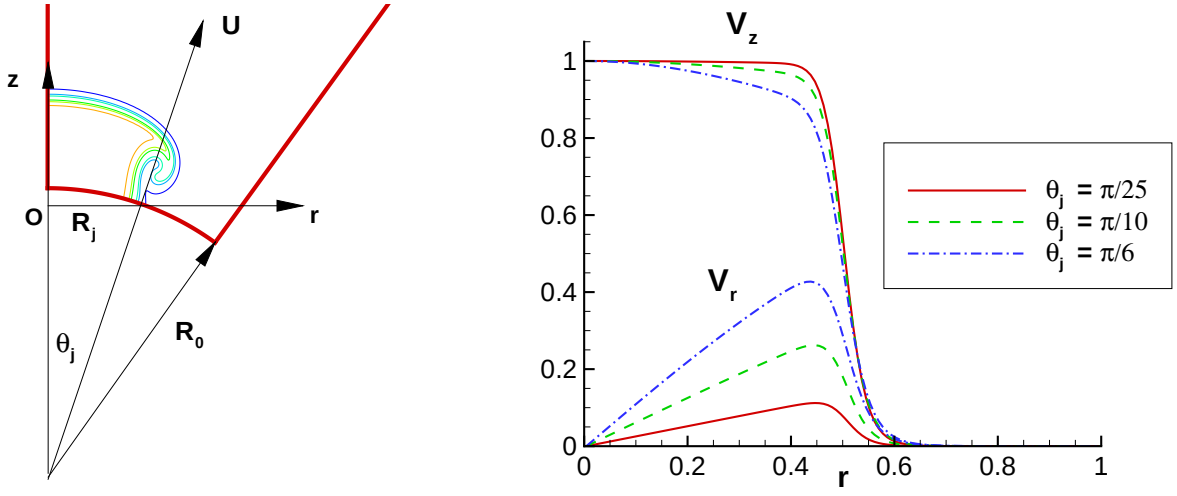

Figure 2: Geometry of the inlet section for the simulation using spherical coordinates (left). Equivalent inflow velocities prescribed at the inlet for the simulation using cylindrical coordinates (right): axial (V_z) and radial (V_r) velocities for different jet injection angles θ_j.

3 NUMERICAL RESULTS

3.1 Cylindrical nozzle

We first compare the two numerical codes when the flow issuing from a cylindrical nozzle is simulated. Since the inflow section is accurately modeled in the CYL-code, the results obtained with this code will be used as reference. We attempt to answer the following fundamental question: how small the jet angle θ_j should be in the simulations with the SPH-code in order to recover the results obtained with the CYL-code? In other words, we attempt to assess for the influence of the curvature of the grid used in the SPH-code on the accuracy of the results.

The answer is offered in Fig. 3 displaying the time evolution of the circulation of the flow $\Gamma = \int\int \omega_\phi$, with ω_ϕ the azimuthal vorticity. The total circulation is an important integral quantity that characterizes the flow and is very sensitive to the inflow velocity condition. It is surprising to see that differences are visible for the jet angle value of $\pi/125$, suggesting that the curvature of the inflow section is still important. Very small values of θ_j are necessary to fully converge to the values obtained with the CYL-code for the same set of parameters and equivalent mesh resolutions.

For $\theta_j = \pi/314$, the inflow section in the SPH-code becomes flat and coincides with the inflow model used in the CYL-code. Using this value of the jet angle, we compare in Fig. 4 the instantaneous fields of vorticity and passive scalar. Almost identical pictures are obtained for both fields.

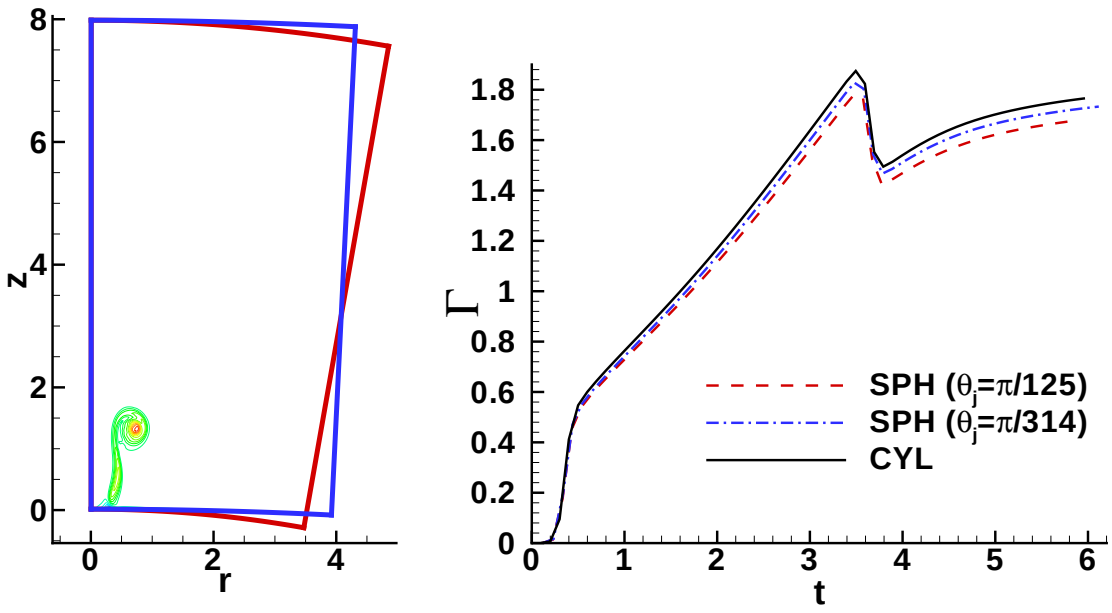

Figure 3: Cylindrical nozzle. Representation of the computational domain for the simulation using spherical coordinates (left). Time evolution of the circulation Γ of the flow (right).

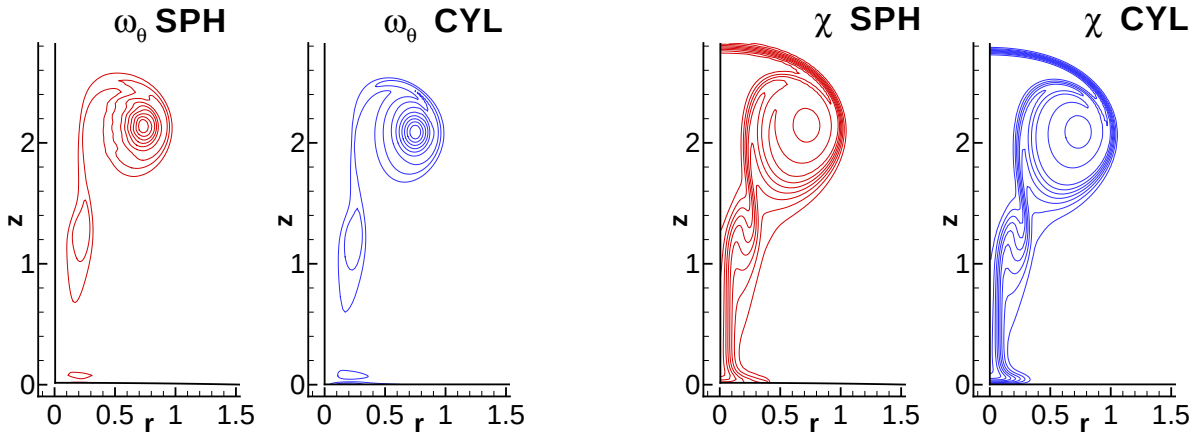

Figure 4: Cylindrical nozzle. Simulations using cylindrical (CYL) and spherical (SPH) coordinates. Instantaneous ($t = 6$) contour lines of the azimuthal vorticity ω_ϕ and passive scalar χ. The SPH simulation uses the value $\theta_j = \pi/314$ for the jet angle.

3.2 Conical nozzle

The injection through conical nozzles proved in engineering applications, but also in biological systems, an effective way to manipulate circulation of the injected slug by controlling the effective exit Reynolds number and exit area[21,22]. An interesting phenomenon in the injected flow is depicted in Fig. 5 for important values of the injection angle θ_j. The slug flow follows the injection angle until the vortex ring rolls-up and acquires sufficient circulation to evolve independently from the slug. It then travels towards the axis of symmetry. The influence of the injection angle is therefore restricted to a small zone near the inflow boundary.

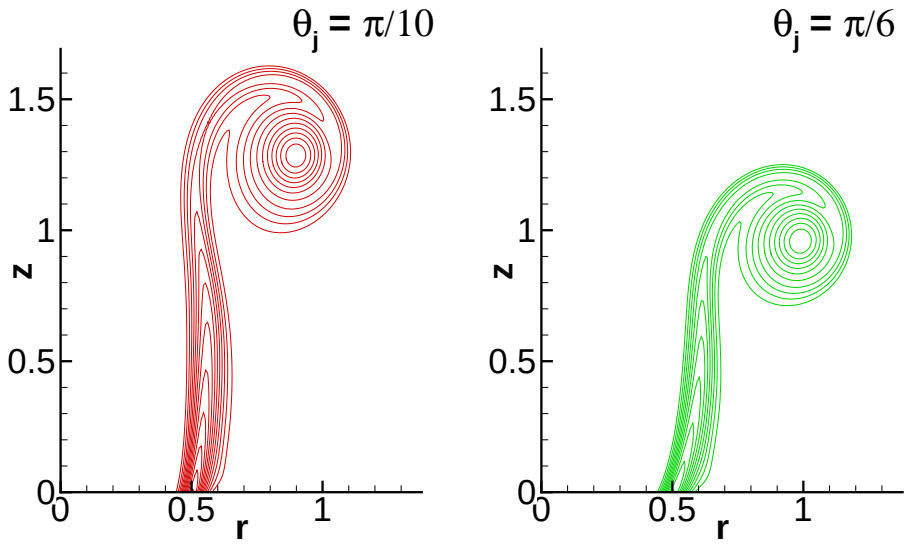

Figure 5: Conical nozzle. Simulations using cylindrical (CYL) coordinates. Instantaneous ($t = 5$) contour lines of the azimuthal vorticity ω_ϕ.

Following this observation, we focus in Fig. 6 on the comparison between the two numerical codes for the early stages of the flow evolution. The circulation of the flow in the SPH simulation grows faster and a stronger vortex ring is obtained. The vortex ring induces an earlier bending of the injected flow towards the axis. This effect is stronger for higher injection angles ($\theta_j = \pi/6$, pictures not shown). The differences in the shape of the vortex rings could also result from the influence of the lateral boundary conditions that allows flow entrainment in the SPH-code. In exchange, the lateral slip-wall in the CYL simulations induces a larger zone of negative vorticity at the inlet section. Separating the effects of the curvature of the computational grid from the influence of the lateral boundary is an interesting issue that needs careful future investigations.

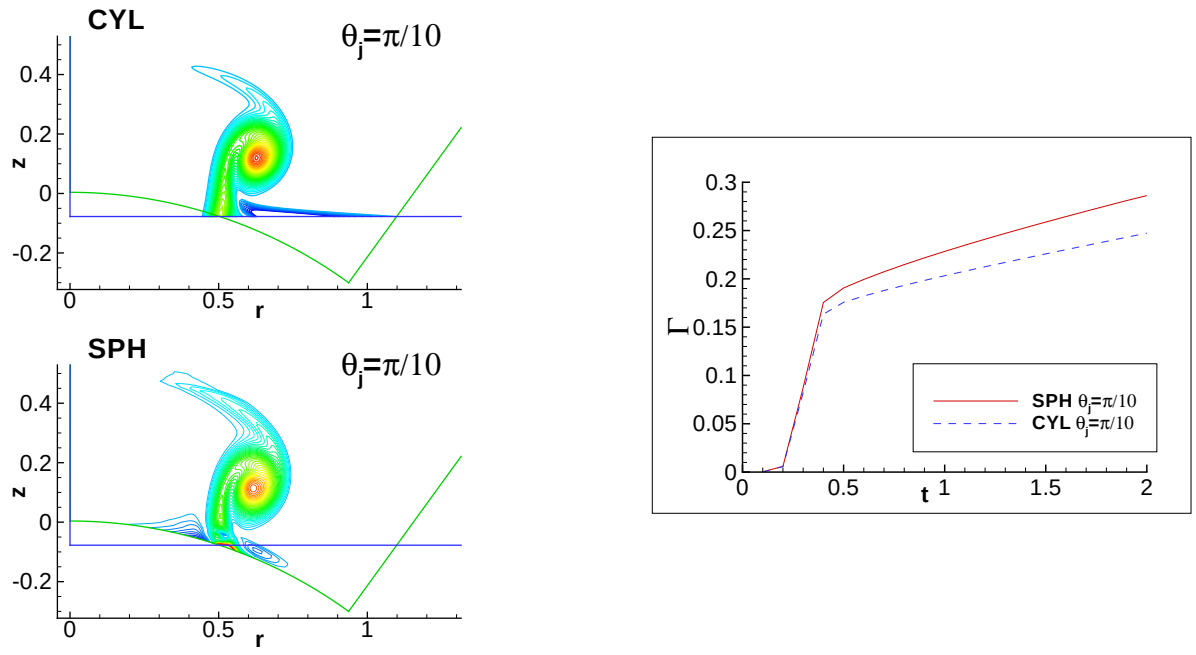

Figure 6: Conical nozzle. Simulations using cylindrical (CYL) and spherical (SPH) coordinates. Instantaneous ($t = 2$) contour lines of the azimuthal vorticity ω_ϕ (left) and time evolution of the flow circulation at early stages of the injection (right).

4 CONCLUSIONS

Two Navier-Stokes solvers using equivalent numerical methods were used to simulate impulsively stated flows from cylindrical and conical nozzles. The equations are discretized using cylindrical (CYL) coordinates in the first code and spherical (SPH) coordinates in the second. The two approaches are well adapted for such simulations, since the axisymmetry of the flow is assumed.

The simulation of laminar vortex rings generated by a cylinder/piston mechanism allowed to quantify the influence of the curvature of the computational grid in the SPH simulation. Using quantitative measurements of the flow circulation, we showed that surprisingly small values of the injection angle ($\theta_j < \pi/125$) are required to recover the results obtained using the CYL approach. Only for such configurations we obtained identical flow patterns from the two numerical codes.

For larger values of the injection angle ($\theta_j = \pi/10$ and $\pi/6$) the reference results were provided by the SPH code. A simple model to prescribe an equivalent velocity at the inlet of the CYL computational domain was derived. Preliminary results showed larger differences in the computed fields than in the case of the cylindrical injection. These results will serve in future investigations to assess for the influence of different numerical parameters (curvature of the grid, influence of the lateral boundary) and will provide a starting point for a full comprehension of the dynamics of the conical injection flow.

Acknowledgements

We are grateful to Prof. B. J. Boersma for providing to us the Navier-Stokes solver using spherical coordinates. S. Danaila acknowledges support from the CNCSIS UEFISCSU, project number PNII IDEI 1030/2007 (contract number 109/2007).

REFERENCES

[1] M. Gharib, E. Rambod, and K. Shariff, A universal time scale for vortex ring formation, *J. Fluid Mech.* **360**, 121 (1998).

[2] M. Hettel, F. Wetzel, P. Habisreuther, and H. Bockhorn, Numerical verification of the similarity laws for the formation of laminar vortex rings, *J. Fluid Mech.* **590**, 35 (2007).

[3] I. Danaila and J. Hélie, Numerical simulation of the postformation evolution of a laminar vortex ring, *Phys. Fluids* **20**, 073602 (2008).

[4] P. S. Krueger, Circulation and trajectories of vortex rings formed from tube and orifice openings, *Physica D* **237**, 2218 (2008).

[5] P. J. Archer, T. G. Thomas, and G. N. Coleman, Passive scalar mixing in vortex rings, *J. Fluid Mech.* **598**, 201 (2008).

[6] S. C. Shadden, K. Katija, M. Rosenfeld, J. E. Marsden, and J. O. Dabiri, Transport and stirring induced by vortex formation, *J. Fluid Mech.* **593**, 315 (2007).

[7] J. O. Dabiri and M. Gharib, Fluid entrainment by isolated vortex rings, *J. Fluid Mech.* **511**, 311 (2004).

[8] I. Danaila, C. Vadean, and S. Danaila, Specified discharge velocity models for the numerical simulation of laminar vortex rings, *Theor. Comput. Fluid Dynamics* **23**, 317 (2009).

[9] B. J. Boersma, Direct numerical simulation of a turbulent reacting jet, in *Ann. Research Briefs*, p. 59, Center for Turbulence Research, Stanford Univ., 1999.

[10] B. J. Boersma, G. Brethouwer, and F. T. M. Nieuwstadt, A numerical investigation on the effect of the inflow conditions on the self similar region of the jet, *Phys. Fluids* **10**, 899 (1998).

[11] I. Danaila and B. J. Boersma, Direct numerical simulation of bifurcating jets, *Physics of Fluids* **12**, 1255 (2000).

[12] A. Hilgers and B. J. Boersma, Optimization of turbulent jet mixing, *Fluid Dyn. Res.* **29**, 345 (2001).

[13] P. Orlandi, *Fluid Flow Phenomena: A Numerical Toolkit*, Kluwer Academic Publishers, Dordrecht, 1999.

[14] M. Rai and P. Moin, Direct Simulations of Turbulent Flow Using Finite–Difference Schemes, *J. Comput. Physics* **96**, 15 (1991).

[15] R. Verzicco and P. Orlandi, A finite–difference scheme for three–dimensional incompressible Flows in cylindrical coordinates, *J. Comput. Physics* **123**, 402 (1996).

[16] S. James and C. K. Madnia, Direct numerical simulation of a laminar vortex ring, *Phys. Fluids* **8**, 2400 (1996).

[17] A. Michalke, Survey on jet instability theory, *Prog. Aerospace Sci.* **21**, 159 (1984).

[18] I. Orlanski, A simple boundary condition for unbounded hyperbolic flows, *J. Comput. Physics* **21**, 251 (1976).

[19] M. R. Ruith, P. Chen, and E. Meiburg, Development of boundary conditions for direct numerical simulations of three–dimensional vortex breakdown phenomena in semi–infinite domains, *Computers & Fluids* **33**, 1225 (2004).

[20] B. J. Boersma, Entrainment Boundary Conditions for Free Shear Flows, *Int. J. Comput. Fluid Dyn.* **13**, 357 (2000).

[21] J. O. Dabiri and M. Gharib, Starting flow through nozzles with temporally variable exit diameter, *J. Fluid Mech.* **538**, 111 (2005).

[22] M. Rosenfeld, K. Katija, and J. O. Dabiri, Circulation Generation and Vortex Ring Formation by Conic Nozzles, *Journal of Fluids Engineering* **131**, 091204 (2009).